FREE VIBRATION ANALYSIS OF A TENSION LEG PLATFORM TENDON

Conference Paper · January 2022

DOI: 10.26678/ABCM.CONEM2022.CON22-0455

3 authors, including:

José Pereira Ramos Junior
Federal University of Piauí
4 PUBLICATIONS **1** CITATION
SEE PROFILE

Simone dos Santos
Federal University of Piauí
31 PUBLICATIONS **79** CITATIONS
SEE PROFILE

CONEM 2022
CONGRESSO NACIONAL DE ENGENHARIA MECÂNICA
TERESINA - PI

ABCM

XI CONGRESSO NACIONAL DE ENGENHARIA MECÂNICA
DE 07 A 11 DE AGOSTO DE 2022, TERESINA-PI, BRASIL

FREE VIBRATION ANALYSIS OF A TENSION LEG PLATFORM TENDON

José Pereira Ramos Junior, josep9957@gmail.com[1]
Brendon Menezes de Abreu, brendon.m.abreu@gmail.com[1]
Simone dos Santos Hoefel, simone.santos@ufpi.edu.br[1]

[1]Federal University of Piauí, Campus Universitário Ministro Petrônio Portella - Ininga, 64049-550, Teresina PI, Brazil

Abstract: *The dynamic behavior in offshore structures is of great importance in the design, conception and operation phase, in order to predict failures, guarantee stability, safety and avoid environmental and financial impacts. An offshore structure consists of a fixing or support plot that departs from the sea soil to the surface of the water and connects to superstructures such as wind turbines, oil and natural gas platforms. In this article, the free vibration of a free-clamped uniform beam, similar to the tendons of a tension leg platform, is studied. Are evaluated beams not immersed and immersed in water, the influence of the dimensions of the cross-sectional and the contribution of the deck as an axial force applied at the free end. Four beam models, Euler-Bernoulli, Rayleigh's, Shear and Timoshenko are used to evaluate natural frequencies using the finite element method. To investigate the influence of axial load, natural frequencies are calculated for various percentages of critical load. The same material parameters are considered in the numerical examples. The results demonstrate that the frequencies obtained by Euler-Bernoulli, Rayleigh and shear surpass those obtained by the Timoshenko theory. In addition, the results indicate that the reduction of the cable cross-section, the influence of water and the contribution of the deck, decrease the natural frequencies of the tendons.*

Keywords: *Offshore, Tension leg platform, Beam theory, natural frequencies, axial force.*

1. INTRODUCTION

Offshore structures are large platforms that primarily provide the necessary facilities and equipment for exploration and production of oil and natural gas in a marine environment. In general, offshore structures may be used for a variety of reasons as: oil and gas exploration; production processing; accommodation; Loading and offloading facilities. There are two main categories of offshore structures, fixed and floating. Fixed structures are designed to withstand environmental forces without substantial displacement. Floating structures are designed to allow small deformations and deflections, but not negligible.

Uściłowska and Kołodziej (1998) provided closed form for a partially immersed cantilever beam with eccentric tip mass. Adrezin and Benaroya (1999), using the Euler-Bernoulli theory and the Morison equation examined the nonlinear transverse behavior of a Tension Leg Platform (TLP) with tension depending on the time due to gravity and buoyancy. Auciello and Ercolano (2004) presented solution for the non-uniform Timoshenko beam to solve the free vibration by the energy method. Wu and Chen (2005) solved the free vibration of non-uniform partially wet Euler-Bernoulli beam with elastic foundation and tip mass.

Wu and Hsu (2007) analyzed the free vibration of partially wet, elastically supported uniform Euler-Bernoulli beam with eccentric tip mass using two separate sets of closed-form solutions for a partially immersed cantilever beam with eccentric tip mass. Wu *et al.* (2010) studied the wave-induced vibrations of an axial-loaded, immersed, uniform Timoshenko beam carrying an eccentric tip mass with rotary inertia using an analytical formulation. De Rosa *et al.* (2013) calculated closed form solution for free vibration of a linearly tapered, partially immersed, elastically supported column with eccentric tip mass. Datta *et al.* (2015) modeled the ocean tower with non-uniform Timoshenko beam, partially submerged, supported by a rigid tip mass with eccentricity at the free end, and non-classical damped foundation on tne other end. In view of the fact that environmental acting in an offshore structure is not static, it becomes important to study the dynamic behavior of the structure. Ankit *et al.* (2016), modeled an ocean tower partially submerged, non-uniform Timoshenko beam having a rigid tip mass with eccentricity at the free end, and non-classical pile foundation at the other end. The pile foundation has been modeled as a distributed spring system which is also known as Winkler Foundation model. The damping effect in the pile-soil interaction was included by using the Kelvin-Voigt model.

The monopile is widely designed as the foundation of offshore wind turbines due to its simplicity (Damgaard *et al.*,

2014; Kuo *et al.*, 2012). A typical monopile is a long hollow steel member with 3-6m outer diameter and 22-40m length (Bisoi and Haldar, 2014), inserted into the sea water and sea bed. It can be regarded as an extension of the wind turbine tower. For such a slender flexible foundation, the interaction between the monopile and the surrounding soil is inevitable and can reduce the vibration frequencies or even vibration modes of the structure, which in turn may further influence the dynamic behaviors of offshore structures (Mostafa and El Naggar, 2004).

In this work, natural frequencies of cantilever beam, circular cross-section, not submerged and submerged in water, similar to a tension-leg platform tendon, are obtained for different diameters values. The influence of axial load applied to the free end is also evaluated. Representing the deck of the offshore structure, different values of axial load are considered. The beam eigenvalues, Euler-Bernoulli (EBT), Rayleigh's (RBT), Shear (SBT), and Timoshenko (TBT) models are obtained using the Finite Element Method (FEM) and the frequency changes between each theory are evaluated.

2. METHODOLOGY

2.1 Classical Theory

The governing coupled differential equations for transverse vibrations of Timoshenko beams are:

$$EI\left(1-\frac{P}{k'GA}\right)v^{iv}+Pv''+\rho A\ddot{v}-\rho I\left(1+\frac{E}{k'G}-\frac{P}{k'GA}\right)\ddot{v}''+\frac{\rho^2 I}{k'G}v^{iv}=0, \tag{1}$$

$$EI\left(1-\frac{P}{k'GA}\right)\psi^{iv}+P\psi''+\rho A\ddot{\psi}-\rho I\left(1+\frac{E}{k'G}-\frac{P}{k'GA}\right)\ddot{\psi}''+\frac{\rho^2 I}{k'G}\psi^{iv}=0, \tag{2}$$

in which E is the modulus of elasticity, I, the moment of inertia of cross-section, k', the shear coefficient, A, the cross-sectional area, G, the modulus of rigidity, ρ the mass per unit volume, P, an initial axial tension load, v, the transverse deflection, ψ the bending slope and the superscripts iv and $\ddot{}$ represent the spatial and temporal derivatives, respectively. Assume that the beam is excited harmonically with a frequency f and

$$v(x,t)=V(x)e^{jft}, \qquad \psi(x)=\Psi(x,t)e^{jft} \qquad \text{and} \qquad \xi=x/L, \tag{3}$$

where $j=\sqrt{-1}$, ξ is the non-dimensional length of the beam, $V(x)$ is normal function of $v(x)$, $\Psi(x)$ is normal function of ψ, and L, the length of the beam. Substituting the above relations into Eq. (1) and Eq. (2) through Eq. (3) and omitting the common term e^{jft}, the following equations are obtained

$$\left(1-p^2s^2\right)\frac{\partial^4 V}{\partial\xi^4}+\left(b^2r^2+b^2s^2-p^2b^2s^2r^2+p^2\right)\frac{\partial^2 V}{\partial\xi^2}+\left(b^4r^2s^2-b^2\right)V=0, \tag{4}$$

$$\left(1-p^2s^2\right)\frac{\partial^4 \Psi}{\partial\xi^4}+\left(b^2r^2+b^2s^2-p^2b^2s^2r^2+p^2\right)\frac{\partial^2 \Psi}{\partial\xi^2}+\left(b^4r^2s^2-b^2\right)\Psi=0, \tag{5}$$

with

$$b^2=\frac{\rho AL^4}{EI}f^2 \qquad \text{and} \qquad f=2\pi\omega, \tag{6}$$

where f is angular frequency, and ω, the natural frequency, and

$$r^2=\frac{I}{AL^2}, \quad s^2=\frac{EI}{k'AGL^2} \quad \text{and} \quad p^2=\frac{PL^2}{EI}, \tag{7}$$

are coefficients related with the effect of rotatory inertia, shear deformation and axial load. The solutions of equations Eq.(4) and Eq.(5) may be written as (Huang, 1961):

$$V(\xi)=C_1 cosh(b\alpha\xi)+C_2 sinh(b\alpha\xi)+C_3 cos(b\beta\xi)+C_4 sin(b\beta\xi), \tag{8}$$

$$\Psi(\xi)=C_1' sinh(b\alpha\xi)+C_2' cosh(b\alpha\xi)+C_3' sin(b\beta\xi)+C_4' cos(b\beta\xi), \tag{9}$$

where the function $V(\xi)$ is know as the normal mode of the beam, C_i and C_i', with $i=1,2,3,4$, are coefficients which can be found from boundary conditions, and α and β are coefficients given as:

$$\alpha=\frac{1}{\sqrt{2}}\sqrt{-(r^2+s^2)+\sqrt{(r^2-s^2)^2+\frac{4}{b^2}}}, \tag{10}$$

$$\beta=\frac{1}{\sqrt{2}}\sqrt{(r^2+s^2)+\sqrt{(r^2-s^2)^2+\frac{4}{b^2}}}. \tag{11}$$

Note that the coefficients r and s relates the four theories of beam, EBT, RBT, SBT, and TBT. On Timoshenko model $r=0$ leads to $\alpha=\alpha_s$ and $\beta=\beta_s$, for $s=0$ the eigenvalues turn to $\alpha=\alpha_r$ and $\beta=\beta_r$, finally for $r=s=0$ we have $\alpha=\beta=\beta_e$.

2.2 The Influence of Water Mass

When a body of mass M moves with a speed Q in a fluid at rest, its kinetic energy T will be (Mason, 1981):

$$T = \frac{1}{2}MQ^2. \tag{12}$$

The existence of this body automatically induces a movement in the fluid around it, which tends to disappear as it the distance that separates it from the body tends to infinity. The law governing the decay of fluid motion depends on the shape of the body and the velocities of the particles $H(x, y, t)$ decreases with $1/r^2$ where r is the distance from the center of the body to the point considered (Pedroso, 1982). The kinetic energy of the fluid surrounding the body that is disturbed T^f will be:

$$T^f = \iint_{lim}^{\infty} \frac{1}{2}\rho H^2(x, y, t)dA, \tag{13}$$

where lim is the limit of body and dA is the elemental area of the body. In this way, the total kinetic energy of the system will be the sum between the kinetic energy of the fluid, Eq.(12) and the kinetic energy of the fluid surrounding the body, Eq. (13), that is:

$$T_{total} = \frac{1}{2}H^2 \left[M + \rho \iint_{lim}^{\infty} \left(\frac{H}{Q}\right)^2 dA \right], \tag{14}$$

in which the second term of the above equation is nothing more than the additional mass M^* this is:

$$M^* = \rho \iint_{lim}^{\infty} \left(\frac{H}{Q}\right)^2 dA. \tag{15}$$

Considering a circular cylinder of radius R submerged by moving in a deep water fluid the additional mass will be:

$$M^* = \rho\pi R^2 L. \tag{16}$$

The additional mass represents the fluid displaced by the movement of the cylinder (Bomtempo and Pedroso, 2016). Thus the natural frequencies for the submerged condition are given by Eq.(17) in which the additional mass is included, that is:

$$\omega_s = b\sqrt{\frac{EI}{(\rho A + M^*)L^4}}. \tag{17}$$

2.3 Finite Element Model

The beam element model is shown in Fig. 1, the generalized coordinates at each node are V, the total deflection, and Ψ, the total slope. This results in an element with four degrees of freedom thus enabling the expression for V and Ψ to contain two undetermined parameters each, which can beam replaced by the four nodal coordinates.

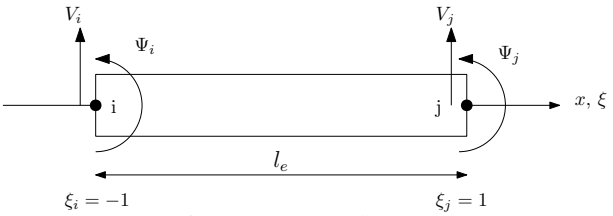

Figure 1: Beam element.

Using the non-dimension coordinate ξ and element length l_e defined in Fig. 1, the displacement V and total slope Ψ can be written in matrix form as follows:

$$V = [\mathbf{N}(\xi)]\{\mathbf{v}\}_e \qquad \text{and} \quad \Psi = \left[\overline{\mathbf{N}}(\xi)\right]\{\mathbf{v}\}_e, \tag{18}$$

where

$$[\mathbf{N}(\xi)] = [N_1(\xi) \quad N_2(\xi) \quad N_3(\xi) \quad N_4(\xi)], \tag{19}$$

$$\left[\overline{\mathbf{N}}(\xi)\right] = [\overline{N}_1(\xi) \quad \overline{N}_2(\xi) \quad \overline{N}_3(\xi) \quad \overline{N}_4(\xi)]. \tag{20}$$

In the current development, a cubic shape and a quadratic shape functions are proposed respectively, as follows:

$$N_i(\xi) = \sum_{i=0}^{3} \lambda_i \xi^i \qquad \text{and} \qquad \overline{N}_i(\xi) = \sum_{i=0}^{2} \overline{\lambda}_i \xi^i, \tag{21}$$

where λ_i and $\bar{\lambda}_i$ are shape functions coefficients. The displacements functions in Eqs.(19) and (20) can be expressed in terms of dimensionless parameters of rotatory r and shear s:

$$\mathbf{N}_i(\xi) = \frac{1}{4(3s^2+1)} \begin{bmatrix} 2(3s^2+1) - 3(2s^2+1)\xi + \xi^3 \\ a[3s^2+1-\xi-(3s^2+1)\xi^2+\xi^3] \\ 2(3s^2+1) + 3(2s^2+1)\xi - \xi^3 \\ a[-3s^2-1-\xi+(3s^2+1)\xi^2+\xi^3] \end{bmatrix}, \tag{22}$$

and

$$\overline{\mathbf{N}}_i(\xi) = \frac{1}{4(3s^2+1)} \begin{bmatrix} a(3\xi^2-3) \\ -1-2(3s^2+1)\xi+6s^2+3\xi^2 \\ a(3-3\xi^2) \\ -1+2(3s^2+1)\xi+6s^2+3\xi^2] \end{bmatrix}, \tag{23}$$

where $a = l_e/2$.

Considering an initial axial load P, the potential energy and kinetic for element length l_e of a uniform beam are given by, respectively:

$$\begin{aligned} \mathbf{U}_e = & \frac{1}{2}\frac{EI}{a}\int_{-1}^{1}\left(\frac{\partial\Psi}{\partial\xi}\right)^2 d\xi + \frac{1}{2}\frac{EI}{as^2}\int_{-1}^{1}\left(\frac{1}{a}\frac{\partial V}{\partial\xi}-\Psi\right)^2 d\xi + \\ & \frac{1}{2}\frac{P}{a}\int_{-1}^{1}\left(\frac{\partial V}{\partial\xi}\right)^2 d\xi, \end{aligned} \tag{24}$$

$$\mathbf{T}_e = \frac{1}{2}\rho Aa\int_{-1}^{1}\left(\frac{\partial V}{\partial t}\right)^2 d\xi + \frac{1}{2}r^2\rho Aa^3\int_{-1}^{1}\left(\frac{\partial\Psi}{\partial t}\right)^2 d\xi. \tag{25}$$

Substituting the displacement expression Eq.(18) into the potential energy Eq.(24) gives:

$$\begin{aligned} U_e = & \frac{1}{2}\{\mathbf{v}\}_e^T\left[\frac{EI}{a}\int_{-1}^{1}[\overline{\mathbf{N}}(\xi)']^T[\overline{\mathbf{N}}(\xi)']d\xi\right]\{\mathbf{v}\}_e + \\ & \frac{1}{2}\{\mathbf{v}\}_e^T\left[\frac{EI}{as^2}\int_{-1}^{1}[\mathbf{N}(\xi)'-\overline{\mathbf{N}}(\xi)]^T[\mathbf{N}(\xi)'-\overline{\mathbf{N}}(\xi)]d\xi\right]\{\mathbf{v}\}_e + \\ & \frac{1}{2}\{\mathbf{v}\}_e^T\left[\frac{P}{a}\int_{-1}^{1}\left[\overline{\mathbf{N}}(\xi)'\right]^T\left[\overline{\mathbf{N}}(\xi)'\right]d\xi\right]\{\mathbf{v}\}_e, \end{aligned} \tag{26}$$

where $[\mathbf{N}(\xi)'] = [\partial\mathbf{N}(\xi)/\partial\xi]$. Therefore, the element stiffness matrix is written by:

$$\begin{aligned} [\mathbf{k}_e] = & \left[\frac{EI}{a}\int_{-1}^{1}[\overline{\mathbf{N}}(\xi)']^T[\overline{\mathbf{N}}(\xi)']d\xi + \right. \\ & \frac{EI}{as^2}\int_{-1}^{1}[\mathbf{N}(\xi)'-\overline{\mathbf{N}}(\xi)]^T[\mathbf{N}(\xi)'-\overline{\mathbf{N}}(\xi)]d\xi + \\ & \left.\frac{P}{a}\int_{-1}^{1}[\mathbf{N}(\xi)']^T[\mathbf{N}(\xi)']d\xi\right]. \end{aligned} \tag{27}$$

Substituting the displacement expression Eq.(18) into the kinetic energy Eq.(25) gives:

$$\mathbf{T}_e = \frac{1}{2}\{\dot{\mathbf{v}}\}_e^T\left[\rho Aa\int_{-1}^{1}[\mathbf{N}(\xi)]^T[\mathbf{N}(\xi)]d\xi + r^2\rho Aa^3\int_{-1}^{1}[\overline{\mathbf{N}}(\xi)]^T[\overline{\mathbf{N}}(\xi)]d\xi\right]\{\dot{\mathbf{v}}\}_e. \tag{28}$$

The element mass matrix is given by:

$$[\mathbf{m}_e] = \left[\rho Aa\int_{-1}^{1}[\mathbf{N}(\xi)]^T[\mathbf{N}(\xi)]\,d\xi + r^2\rho Aa^3\int_{-1}^{1}\left[\overline{\mathbf{N}}(\xi)\right]^T\left[\overline{\mathbf{N}}(\xi)\right]d\xi\right]. \tag{29}$$

3. NUMERICAL RESULTS

This section presents three numerical examples involving TBT, SBT, RBT and EBT. First, the validation of the present model is presented, then the natural frequencies are calculated for a non-submerged and submerged beam. In order to investigate the influence of axial load, natural frequencies are calculated for various percentages of critical load for a non-submerged clamped-free beam.

A circular cross-section beam such that $L = 2\,\mathrm{m}$, $d = 0.05\,\mathrm{m}$, $\kappa = 3/4$, $E = 206.8\,\mathrm{GPa}$, $\rho = 7850\,\mathrm{kg/m^3}$, $\nu = 0.3$ and axial load P is used, Fig. 2, where L is the beam length, d the diameter of the cross-section, k the shear correction

factor, E the modulus of elasticity, ρ the specific mass, ν Poisson's ratio and P is the axial load defined as a percentage of the load criticizes. The TBT includes all the portions of energy involved in the free vibration of this structure, being sufficient to validate the model. The results were obtained by FEM (discretization with 50 and 70 elements). The values of rotational inertia and shear deformation factors are, respectively, $r = 1$ and $s = 1$. This example is presented by Wu (2013).

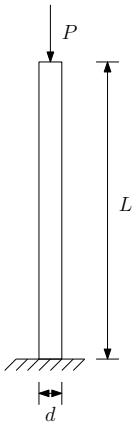

Figure 2: Clamped-free beam subjected to an axial load.

Table 1 compares the natural frequencies presented by Wu (2013) analytically and those obtained by the author using the FEM, for different percentages η of the critical load.

Table 1: Eigenvalues of the clamped-free beam.

Axial load $-\boldsymbol{\eta} = \mathbf{0}$					
Eigenvalues	Exact (Wu, 2013)	FEM (50 elem)	Error (%)	FEM (70 elem)	Error (%)
$\omega_1(\mathrm{rad/s})$	56.3723	56.3722	1.7739e-4	56.3722	1.7739e-4
$\omega_2(\mathrm{rad/s})$	352.4269	352.4300	8.7962e-4	352.4271	5.6749e-5
$\boldsymbol{\omega}_3(\mathrm{rad/s})$	982.9945	983.0619	6.8566e-3	982.9988	4.3744e-4
Axial load $-\boldsymbol{\eta} = \mathbf{0.9}$					
Eigenvalues	Exact (Wu, 2013)	FEM (50 elem)	Error (%)	FEM (70 elem)	Error (%)
$\boldsymbol{\omega_1}(\mathrm{rad/s})$	18.4651	18.46504	3.2494e-4	18.46504	3.2494e-4
$\boldsymbol{\omega}_2(\mathrm{rad/s})$	325.0698	325.0701	9.2288e-5	325.0699	3.0763e-5
$\boldsymbol{\omega}_3(\mathrm{rad/s})$	960.4208	960.4289	8.4338e-4	960.4246	3.9566e-4

With 50 finite elements, Tab. 1, the natural frequencies obtained by the FEM are already satisfactorily close to the analytical frequencies presented by Wu (2013).

The tendon is modelled a beam of circular cross-section such that $L = 100\,\mathrm{m}$, $d = 0.3\,\mathrm{m}$, $k = 3/4$, $E = 206.8\,\mathrm{GPa}$, $\rho = 7850\,\mathrm{kg/m^3}$, $\nu = 0.3$, $\rho_{water} = 1000\,\mathrm{kg/m^3}$ is considered, Fig. 3. These numerical values are adapted from Wu (2013) and Bomtempo and Pedroso (2016). The values of the rotational inertia and shear deformation factors are, respectively, $r = 0$ and $s = 0$, for EBT, $r = 1$ and $s = 0$ for RBT, $r = 0$ and $s = 1$ for SBT, and $r = 1$ and $s = 1$ for TBT. The results are obtained by FEM (discretization with 50 elements).

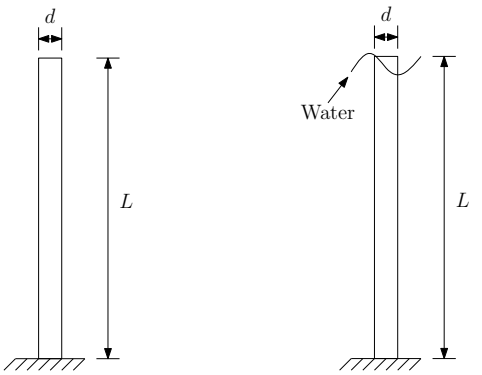

(a) Non-submerse. (b) Submerse.

Figure 3: Clamped-free beam Non-submerse and Submerse.

Table 2 presents the first three natural frequencies for the submerged tendon, Fig. 3a, and non-submerged, Fig. 3b, obtained by the four beam theories, with diameters of $0.3\,\mathrm{m}$ and $0.15\,\mathrm{m}$

Table 2: Eigenvalues of the clamped-free beam.

Non-submerse beam $-\,\mathbf{d = 0.3\ m}$				
Frequencies (rad/s)	TBT	SBT	RBT	EBT
ω_1	0.135347	0.135348	0.135348	0.135348
ω_2	0.848178	0.848186	0.848205	0.848213
ω_3	2.374791	2.374842	2.374969	2.375021
Submerse beam $-\,\mathbf{d = 0.3\ m}$				
Frequencies (rad/s)	TBT	SBT	RBT	EBT
ω_1	0.127472	0.127472	0.127472	0.127472
ω_2	0.798822	0.798830	0.798848	0.798855
ω_3	2.236601	2.236650	2.236769	2.236818
Non-submerse beam $-\,\mathbf{d = 0.15\ m}$				
Frequencies (rad/s)	TBT	SBT	RBT	EBT
ω_1	0.067674	0.067674	0.067674	0.067674
ω_2	0.424102	0.424103	0.424105	0.424106
ω_3	1.187482	1.187488	1.187504	1.187510
Submerse beam $-\,\mathbf{d = 0.15\ m}$				
Frequencies (rad/s)	TBT	SBT	RBT	EBT
ω_1	0.063736	0.063736	0.063736	0.063736
ω_2	0.399423	0.399424	0.399427	0.399428
ω_3	1.118382	1.118388	1.118403	1.118409

The diameter decrease from $0.3\,\mathrm{m}$ to $0.15\,\mathrm{m}$ leads to a decrease in natural frequencies, the same effect is observed including the water. Any of the four theories present satisfactory results due to the proximity of the frequency values.

Table 3 shows the first three natural frequencies for the non-submerged tendon obtained by the four beam theories, with diameters of $0.3\,\mathrm{m}$. In this case an axial load that represents the influence of the deck on the tendon stiffness, Fig. 2, η varies from 0 to 0.9 which corresponds to the percentage of the critical load applied to the structure.

Table 3: Eigenvalues of the clamped-free beam with axial load.

Axial load - $\boldsymbol{\eta = 0}$				
Frequencies (rad/s)	TBT	SBT	RBT	EBT
$\boldsymbol{\omega_1}$	0.135347	0.135348	0.135348	0.135348
$\boldsymbol{\omega_2}$	0.848184	0.848192	0.848210	0.848218
$\boldsymbol{\omega_3}$	2.374914	2.374966	2.375090	2.375142
Axial load - $\boldsymbol{\eta = 0.3}$				
Frequencies (rad/s)	TBT	SBT	RBT	EBT
$\boldsymbol{\omega_1}$	0.114523	0.114523	0.114523	0.114524
$\boldsymbol{\omega_2}$	0.826925	0.826932	0.826951	0.826959
$\boldsymbol{\omega_3}$	2.356996	2.357047	2.357172	2.357223
Axial load - $\boldsymbol{\eta = 0.6}$				
Frequencies (rad/s)	TBT	SBT	RBT	EBT
ω_1	0.087630	0.087630	0.087630	0.087630
ω_2	0.805046	0.805053	0.805073	0.805080
ω_3	2.338939	2.338990	2.339116	2.339167
Axial load - $\boldsymbol{\eta = 0.9}$				
Frequencies (rad/s)	TBT	SBT	RBT	EBT
ω_1	0.044394	0.044394	0.044395	0.044395
ω_2	0.782512	0.782519	0.782539	0.782546
$\boldsymbol{\omega_3}$	2.320743	2.320794	2.320921	2.320971

The parameter $\eta = 0$ in Tab. 3, corresponds to the absence of axial load, which coincides with the case of Tab. 2 with a diameter of $0.3m$ and not immersed in water. In this particular case note that the two tables have the same values of frequency. For the other values of η in Tab. 3, it is observed that the increase in the axial load value reduces the natural frequencies.

The EBT representing pure bending, considers kinetic energy due to translation inertia and potential energy due to bending. In RBT as a sophistication of EBT, kinetic energy due to rotation inertia is also considered, as a result of this addition of energy the frequencies in RBT were lower than EBT. In SBT the two energy parcels present in EBT and the potential energy due to shear are considered, then the frequencies obtained were lower than in RBT, consequently lower than in EBT. In TBT, the four energy parcels are considered to be the most sophisticated model, with values more consistent with physical problems, in this case the frequencies were the lowest among the four beam theories. Therefore, EBT, RBT and SBT overestimate natural frequencies.

4. CONCLUSION

The tendon of a TLP structure was modeled after the four beam theories. Using the finite element method, natural frequencies were obtained for different values of cross-sectional area. The influence of water and the deck on the frequencies of the tendon were evaluated.

It was observed that EBT, RBT and SBT surpass the frequencies obtained by TBT. It has been shown that the decrease in cross section, as well as the inclusion of the water mass, decreases natural frequencies. It was also observed the effect of the deck on the tendon stiffness, represented by the axial load at the free end, slightly decreases the natural frequencies as the value of the applied load increases.

5. REFERENCES

Adrezin, R. and Benaroya, H., 1999. "Non-linear stochastic dynamics of tension leg platforms". *Journal of Sound and vibration*, Vol. 220, No. 1, pp. 27–65.

Ankit, A., Datta, N. and Kannamwar, A.N., 2016. "Free transverse vibration of mono-piled ocean tower". *Ocean Engineering*, Vol. 116, pp. 117–128.

Auciello, N. and Ercolano, A., 2004. "A general solution for dynamic response of axially loaded non-uniform timoshenko beams". *International Journal of Solids and structures*, Vol. 41, No. 18-19, pp. 4861–4874.

Bisoi, S. and Haldar, S., 2014. "Dynamic analysis of offshore wind turbine in clay considering soil–monopile–tower interaction". *Soil Dynamics and Earthquake Engineering*, Vol. 63, pp. 19–35.

Bomtempo, T.B.S. and Pedroso, L.J., 2016. "Um estudo analítico-numérico da influência do deck no comportamento dinâmico de uma plataforma offshore mono leg em vibraoções livres". *Revista Interdisciplinar de Pesquisa em Engenharia*, Vol. 2, No. 24, pp. 246–254.

Damgaard, M., Zania, V., Andersen, L.V. and Ibsen, L.B., 2014. "Effects of soil–structure interaction on real time dynamic response of offshore wind turbines on monopiles". *Engineering Structures*, Vol. 75, pp. 388–401.

Datta, N. *et al.*, 2015. "Free transverse vibration of ocean tower". *Ocean Engineering*, Vol. 107, pp. 271–282.

De Rosa, M., Lippiello, M., Vairo, F. and Maurizi, M., 2013. "Free vibration analysis of a variable cross-section column partially immersed in a liquid". *Ocean engineering*, Vol. 72, pp. 160–166.

Huang, T., 1961. "The effect of rotatory inertia and of shear deformation on the frequency and normal mode equations of uniform beams with simple end conditions". *J. Appl. Mech*, Vol. 28, No. 4, pp. 579–584.

Kuo, Y.S., Achmus, M. and Abdel-Rahman, K., 2012. "Minimum embedded length of cyclic horizontally loaded monopiles". *Journal of Geotechnical and Geoenvironmental Engineering*, Vol. 138, No. 3, pp. 357–363.

Mason, J., 1981. *Obras portuárias*. Editora Campus.

Mostafa, Y.E. and El Naggar, M.H., 2004. "Response of fixed offshore platforms to wave and current loading including soil–structure interaction". *Soil Dynamics and Earthquake Engineering*, Vol. 24, No. 4, pp. 357–368.

Pedroso, L., 1982. "Alguns aspectos da interação fluido-estrutura em estruturas off-shore". *Dissertação de Mestrado*.

Uściłowska, A. and Kołodziej, J., 1998. "Free vibration of immersed column carrying a tip mass". *Journal of Sound and Vibration*, Vol. 216, No. 1, pp. 147–157.

Wu, J.S., 2013. *Analytical and numerical methods for vibration analyses*. John Wiley & Sons.

Wu, J.S. and Chen, C.T., 2005. "An exact solution for the natural frequencies and mode shapes of an immersed elastically restrained wedge beam carrying an eccentric tip mass with mass moment of inertia". *Journal of Sound and Vibration*, Vol. 286, No. 3, pp. 549–568.

Wu, J.S., Chen, C.T. *et al.*, 2010. "Wave-induced vibrations of an axial-loaded immersed timoshenko beam carrying an eccentric tip mass with rotary inertia". *Journal of ship research*, Vol. 54, No. 1, pp. 15–33.

Wu, J.S. and Hsu, S.H., 2007. "The discrete methods for free vibration analyses of an immersed beam carrying an eccentric tip mass with rotary inertia". *Ocean Engineering*, Vol. 34, No. 1, pp. 54–68.

6. COPYRIGHT RESPONSIBILITY

The authors confirm that they are solely responsible for the authorship of this work and that all material included herein as part of this work is the property (and authorship) of the authors, or has the owners' permission to be included here.